Available online at www.sciencedirect.com
ScienceDirect
Mendeleev Commun., 2008, **18**, 38–41
Mendeleev Communications

Zeta-potential and morphology of electrospun nano- and microfibers from biopolymers and their blends used as scaffolds in tissue engineering

Cedryck Vaquette,[a] Valery G. Babak,*[b,c] Francis Baros,[b] Omar Boulanouar,[d] Dominique Dumas,[e] Patrick Fievet,[f] Natalia R. Kildeeva,[g] Philippe Maincent[h] and Xiong Wang[a]

[a] *Groupe Bioingénierie, LEMTA, Nancy-Université, CNRS, 54500 Vandoeuvre-les-Nancy, France*
[b] *Département de Chimie Physique des Réactions, UMR 7630 CNRS-INPL, Groupe ENSIC, 54000 Nancy, France*
[c] *A. N. Nesmeyanov Institute of Organoelement Compounds, Russian Academy of Sciences, 119991 Moscow, Russian Federation. Fax: +7 499 135 5085; e-mail: babak@ineos.ac.ru*
[d] *LMN-AC, UMR CEA E4, Université de Franche-Comté, 25030 Besançon, France*
[e] *IFR 111 LEMTA, Nancy-Université, CNRS, Faculté de Médecine, 54505 Vandoeuvre-les-Nancy, France*
[f] *Institut UTINAM (UMR CNRS 6213), Equipe 'Nanosciences, Capteurs, Membranes' UFR Sciences et Techniques, 25030 Besançon, France*
[g] *A. N. Kosygin Moscow State Textile Academy, 117918 Moscow, Russian Federation*
[h] *Laboratoire de Pharmacie Galénique, Faculté de Pharmacie, Université Henri Poincaré, 54001 Nancy Cédex, France*

DOI: 10.1016/j.mencom.2008.01.015

The effect of the composition of the blend of hydrophobic biopolymers onto zeta-potential and morphology of electrospun nano- and microfibers has been investigated.

Electrostatic spinning or electrospinning is a fiber spinning technique driven by a high-voltage electric field that produces fibers with diameters in a submicrometer to nanometer range.[1] Nanofibers are typical one-dimensional colloidal objects with an increased tensile strength, whose length can achieve a few kilometers and the specific surface area can be 100 $m^2\ g^{-1}$ or higher.[2]

Nano- and microfibers from biocompatible polymers and biopolymers have received much attention in medical applications[3] including biomedical structural elements (scaffolding used in tissue engineering,[2,4–6] wound dressing,[7] artificial organs and vascular grafts[8]), drug and vaccine delivery,[9–11] protective shields in speciality fabrics, multifunctional membranes, *etc*. Other applications concern superhydrophobic coatings,[12] encapsulation of solid materials,[13] filter media for submicron particles in separation industry, composite reinforcement and structures for nano-electronic machines.

The thickness and morphology of electrospun fibers obtained from polymer solutions depend on the physico-chemical properties of these solutions such as viscosity, conductivity, dielectric constant, boiling point, and surface tension, as well as on the technological parameters: flow rate of the solution from the capillary, applied electric potential and distance between the tip and the collector (Figure 1).[2,14,15] The surface properties of these fibers, *e.g*., the zeta-potential in an aqueous phase, depend on the type and surface density of ionizable or polar functional groups of polymers, *i.e.*, on the type of polymers used.

Previously, by producing nanocapsules for pharmaceutical use from the hydrophobic biopolymers, it has been shown that poly(ε-caprolactone) (PCL) provides a negative zeta-potential to these nanoparticles, whereas the nanoparticles obtained from Eudragit RS (a polymethacrylate-based copolymer containing ~2 mol% of trimethylammonium groups) are always positively charged.[16,17] The nanoparticles obtained from the blends of PCL and Eudragit RS have positive zeta-potential for the blends

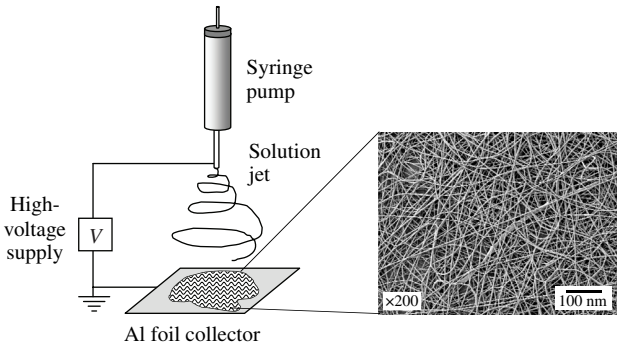

Figure 1 Schematic sketch of the electrospinning setup used for fabricating stochastic microfibrous mats.

with the composition φ = [PCL]/[PCL + Eudragit RS] ≤ 0.8 exhibiting asymmetry of surface electric charge with regard to the polymers composition in blend.[18] This feature has been explained by a higher polarity and surface activity of Eudragit RS with regard to PCL, and by a lower solubility of the former polymer in dichloromethane.[19]

We supposed that the zeta-potential and morphology of electrospun nano- and microfibers could be controlled using the blends of polymers with different polar and ionisable groups, such as PCL and Eudragit RS. The aim of this study was to control the surface properties of nano- and microfibrous membranes used as scaffolds in tissues engineering and as highly selective adsorbents for polyelectrolytes.[†]

The measurements of the zeta potentials of polymeric fibers were performed with a ZETACAD (CAD Inst., France) zeta meter using a cylindrical glass cell for fibrous or granular samples. This apparatus measures the electrical potential difference generated by the imposed movement of an electrolyte solution through a fiber plug. The liquid is forced through the fiber plug using nitrogen gas and its pressure is controlled by a pressure

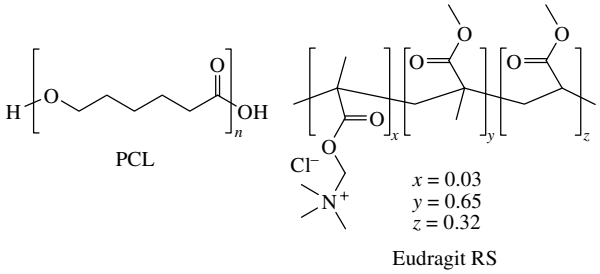

Figure 2 Chemical structure of biopolymers.

sensor. The cell is mounted between a pair of Ag/AgCl wire electrodes linked to a Keithley multimeter (model 2000) to measure the electrical potential difference ($\Delta\varphi_s$) between the plug ends.[21,22]

The zeta-potential (ζ) was determined by the Smoluchowski equation

$$\zeta = \frac{\Delta\varphi_s}{\Delta P}\frac{\eta\lambda_0}{\varepsilon_0\varepsilon_r}, \quad (1)$$

where ΔP is the applied pressure, η is the dynamic viscosity of the measuring fluid, λ_0 is the conductivity, ε_r and ε_0 are the dielectric constant and vacuum permittivity, respectively. The surface conductivity of fibrous samples was ignored. The streaming potential was measured in a 10^{-3} M KCl solution at pH 5.7±0.1.

The surface potentials of the Langmuir layers of polymers were studied with a KSV Minithrough (Finland) equipped with a surface potential measurement device.[19]

The morphology of the fibers depends on the polymers and the physico-chemical conditions (Figure 3). The higher diameters of fibers were obtained for PCL solutions [Figure 3(*a*)], whereas the fibers with smaller diameters were produced from pure Eudragit RS solutions [Figure 3(*c*)]. The decrease of the fiber diameter correlates with the viscosity of polymer solutions decreasing in the order PCL > PCL/Eudragit RS > Eudragit RS.[17,19] This feature was reported for other hydrophobic polymers (PCL, PLGA, PLLA, PLA, *etc.*).[2,14,23–25] Note that, in the case of PCL, two sizes of fibers are produced: one microscopic with a diameter of around 5 μm and another one nanoscopic with diameters of around 400 nm or lower [Figure 3(*a*)]. This phenomenon occurs in high viscosity solutions with a relatively low electrical conductivity above a critical value of the electrostatic field.[1,14]

As concerned the blends of the PCL with the Eudragit RS, the electrospinning of the DCM solutions gives fibers with almost the same microscopic diameters about 1–2 μm as have the Eudragit RS fibers [Figure 3(*b*)]. At the same time, the bulk viscosity of the mixed solution containing only 4 wt% Eudragit RS is almost the same as the viscosity of the PCL solution and considerably higher than the viscosity of individual Eudragit RS solutions of the same or even higher bulk concentration.[17] Consequently, the proportionality between the fiber diameters and the viscosity[2,14,23–25] does not hold in the case of the blends of polymers. The origin of this feature may be a higher electrical conductivity of the blend with regard to the individual PCL solution due to the ionic conductivity of Eudragit RS. The decrease of the fiber diameters with increasing electrical conductivity of jets was reported.[14]

In this connection, it is interesting that a similar spectacular decrease of the size of nanoparticles made from the PCL was observed upon addition to the PCL solution of at least of ~15 wt% Eudragit RS.[19] With further increase of the Eudragit RS content in the blend, the nanoparticle size did not decrease remaining equal to that corresponding to pure Eudragit RS. This property has been explained by the proved preponderant effect of the interfacial tension γ over the viscosity η of polymer solutions in DCM on the work of emulsification of DCM solutions in water. Because of the concentration of TMA groups at the surface, the interfacial tension γ of blends decreased to the values which were almost equal to that of Eudragit RS solutions; thereby, the nanoparticles made of the PCL/Eudragit RS blend acquired the same small size as those made from pure Eudragit RS. It seems that in the case of the fibers the role of the surface properties of the solutions (surface tension and electric conductivity) plays a determinant role in the thinning of fibers in an electrical field. However, the detection and quantification of these surface properties is difficult under fast non-equilibrium conditions of

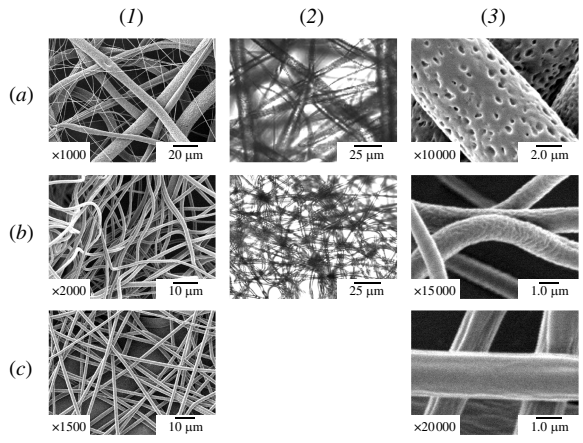

Figure 3 (*1*, *3*) SEM and (*2*) confocal fluorescence micrographs of the fibers from biopolymers and their blends. (*a*) PCL; (*b*) PCL/Eudragit RS; (*c*) Eudragit RS.

† PCL (80 000 g mol^{-1}) from Sigma Aldrich, Eudragit RS (150 000 g mol^{-1}) from Degussa (Figure 2), rhodamine B isothiocyanate (RBITC) from Fluka and dichloromethane (DCM) of analytical grade from Sigma Aldrich were used. Water was purified using a Milli-Q plus 185 system (Millipore).

Solutions of PCL, Eudragit or the blend PCL-Eudragit (96/4 wt%) in DCM were employed to produce nano- and microfibers. The concentrations of polymers in DCM have been adjusted on account for the viscosity of these solutions, and their compatibility in DCM. The concentrations (wt/vol) of individual PCL and Eudragit RS were 14 and 50%, respectively, whereas that for their blend was equal to 16%. The viscosity of polymer solutions was determined using an Ubhellode viscosimeter with a glass capillary at 20 °C.

The phase diagram of the PCL–Eudragit RS–methylene chloride ternary system was constructed *via* determination of the turbidity (at λ = 400 nm) of mixed 5% solutions with different PCL/Eudragit ratios in the process of solvent evaporation.

The electrospinning machine was composed by a syringe pump, a 10 ml glass syringe and a flexible plastic rod connected to a 20G needle (Figure 1). The electrostatic field was produced by a high-voltage power unit (Heizinger, Germany). The collector consisted of a plane aluminum sheet (to produce a stochastic microfiber membrane). Depending on the polymer solution viscosity and conductivity, the applied electric potential varied in the range 10–15 kV, whereas the air gap (the distance between the needle and the Al sheet) was fixed at 10–15 cm. The polymer solution flow rate was 2 ml h^{-1}, and the experiments were performed at 18 °C.

The surface morphology of the fibers was investigated using a Cambridge scanning electron microscope at 20 kV. The fibrous membranes were gold–palladium coated before observation.

For the images series of fiber internal morphology and structure, a Leica TCS SP2-AOBS confocal microscope (Leica Microsystems, Germany) equipped with an acousto-optical beamsplitter, an 100 mW argon laser (457, 476, 488 and 514 nm) and a Helium Neon laser (543 and 633 nm) and a 8 W VERDI laser MIRA 900F (from 600 to 1100 nm, Coherent, France) were respectively used with an ×40/0.8 water immersion.[20] At 543 nm excitation, the bandwidths of the detected fluorescence wavelengths were optimised for each channel to a maximum emission (582–651 for rhodamine). Fluorescence emissions were recorded within an Airy disk confocal pinhole setting fully closed (1 A) and images at a 0.238 μm (*x*,*y*) pixel size were obtained for each case in 512×512 matrices.

the solidification of a liquid jet during solvent evaporation.

In the case of PCL fibers, the surface contains holes in the form of craters with diameters of 100–500 nm [Figure 3(*a*)]. This effect is well known in the formulation of polymeric microparticles by solvent evaporation and is explained by the instability of the diffusion flux of DCM, which transforms to numerous convection nanofluxes during the excessively rapid evaporation of the solvent through the surface.[26] The higher is the viscosity of the medium, the more probable is this instability of the diffusion flux and the appearance and subsistence of the craters. Less viscous solutions of pure Eudragit RS lead to perfectly smooth fibers and nanoparticles exempt of the craters [Figure 3(*c*)]. On the other hand, the surface of the PCL/Eudragit RS fibers presents nanoscaled roughness with a brain-like morphology [Figure 3(*b*)]. Identical and even more pronounced morphology exhibit nanoparticles made from the same PCL/Eudragit RS blend.[27]

Previously, it has been demonstrated that the nano-roughness of the surfaces of polymeric particles provides from the phase separation in the mixed solution inside the sub-surface layers at the skin of nanoparticles during solvent evaporation when the lesser soluble in the DCM cationic polymer Eudragit RS separates from the solution in the form of nano-clusters.[27] Moreover, during evaporation the frontal flux of the solvent moves these nano-clusters towards the surface by the diffusio-phoresis, and finally the PCL remained in the central core, whereas the clusters of Eudragit RS formed an exterior shell. This effect has been proved by the covalent grafting to Eudragit RS of rhodamine that makes visible the cluster structure by confocal laser scanning microscopy (CLSM).[18] In this study, we used the same strategy to detect the same effect of the segregation and the spatial separation of two polymers inside the fiber, particularly the preferential location of coloured Eudragit RS at the skin of the fiber [Figure 3(*b*)]. Unfortunately, this effect was too small although the rough brain-like morphology of the surface and the positive electric charge of the fiber surface testify for some exceeding concentration of Eudragit RS at the surface with regard to the core of the fibers.

The above effect of phase segregation can be explained by the rapid solvent evaporation during the deposition of fibers. The Eudragit RS clusters born as the consequence of increasing the local polymer concentration in the bulk of the jet have insufficient time to displace by diffusio-phoresis towards the surface of the fiber. This evaporation rate could be eventually decreased in some limits by increasing the flow rate of the polymer solution or/and by decreasing the air gap.[28,29] In these cases, the solvent will not have sufficient time to totally evaporate leading to the deposition of wet fibers. By such a way, by producing the fibers with larger diameters, we expect to produce conditions for a more pronounced segregation effect.

The streaming potential $\Delta\varphi_s$ measurements (Figure 4) of the fibers made from the pure polymers, PCL (curve *1*) and Eudragit RS (curve *3*), show that the zeta-potential of the PCL fibers calculated using equation (1) is negative, $\zeta_{PCL} = -28$ mV, whereas that of the Eudragit RS fibers shows a positive value $\zeta_{Eud} = +78$ mV. This is quite expected result while for the nanoparticles prepared from the same pure polymers we have found the same polarity and zeta-potentials.[19] The positive sign of the zeta potential of Eudragit RS fibers is due to the ionization of cationic TMA groups in the aqueous phase that leads to the formation of double layers of ions. In the case of the PCL fibers, the negative charge of the surface may be explained by the orientation of carbonyl groups of this compound at the surface (Figure 4).

This preponderant orientation of carbonyl groups in contact with the aqueous phase was found by the measurement of the surface potential ΔV of PCL Langmuir monolayers obtained by spreading PCL solutions in DCM.[19] $\Delta V \sim 0.4$ V for the liquid condensed (LC) state of these monolayers is due to the cumulative effect of dipole moments of the carbonyl groups at the surface equal to $\mu_{C=O} = 2.7$ D. On the other hand, the surface potential for the Eudragit RS Langmuir monolayers acquired the high value $\Delta V \sim 0.8$ V due to the cumulative contribution of the effective dipole moments μ_{TMA} of ionised cationic TMA groups with their counter ions.

Table 1 Zeta-potentials of the fibers.

Fiber	Zeta-potential/mV
PCL	−28±1
PCL–Eudragit	+24±3
Eudragit	+75±2

The positive sign of the zeta-potential of the fibers made from the PCL/Eudragit RS blend is due to the preponderant concentration of TMA groups of the Eudragit RS at the surface that neutralises the electric champs provided from the carbonyl groups of the PCL. It is significant that only 4 wt% Eudragit RS in the blend produces this drastic variation of the zeta-potential sign from negative to positive. The positive surface charge and the nano-roughness of the fiber surface [Figure 3(*b*)] testifies for the phase separation in the blend and the formation of Eudragit RS clusters near the fiber surface that is in the origin of the Eudragit RS concentration at the surface.

Usually, the modification of the surface properties of the fibers is proceeded by the covalent grafting of functional groups (*e.g.*, carboxyl groups[30]) after the electrospun process. The hydrolysis of PCL, PLA and polyesters leads to the appearance of COOH and OH groups at the fiber surface.[31,32] The control of the surface electric charge of electrospun nano- and microfibers using polymers with corresponding functional groups, *e.g.*, carbonyl, carboxyl, TMA and amino groups, and their mixtures, offers a facile and inexpensive way of preparing effective

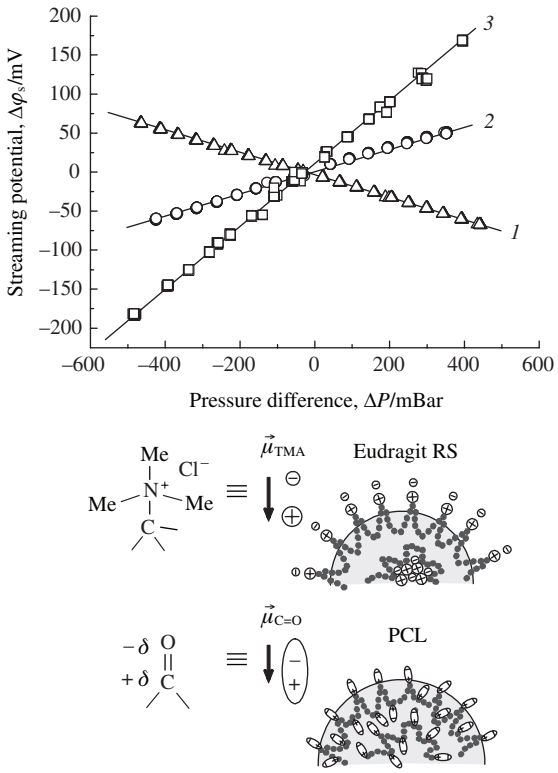

Figure 4 Streaming potential ($\Delta\varphi_s$) as a function of pressure difference (ΔP) for the fibers made from (*1*) PCL, (*2*) PCL/Eudragit RS and (*3*) Eudragit RS in a 10^{-3} M KCl solution at pH 5.7±0.1.

scaffolds for tissue engineering with controlled adhesive characteristics.[4] Another application of such fibers having different surface potential and relatively low hydrodynamic resistance for the filtration may be the formulation of adsorbents for polyelectrolyte separation.

This work was supported by the CNRS and the Région Lorraine (ATIP/SPI and scholarship for C.V.). We are grateful to Mrs. M.-J. Belgy and Mr. J.-F. Rémy for SEM imaging. V. B. thanks the CNRS for his invited professor position in INPL of Nancy.

References

1 S. Ramakrishna, K. Fujihara, W. E. Teo, T. C. Lim and Z. Ma, *An Introduction to Electrospinning and Nanofibers*, World Scientific Publishing Co. Pte. Ltd., London, 2005.
2 I. K. Kwon, S. Kidoaki and T. Matsuda, *Biomaterials*, 2005, **26**, 3929.
3 G. Buschle-Diller, A. Hawkins and J. Cooper, in *Modified Fibers with Medical and Specialty Applications*, eds. J. V. Edwards, G. Buschle-Diller and S. C. Goheen, Springer, Dordrecht, Neth CODEN: 69ICLQ Conference, 2006.
4 C. Vaquette, S. Fawzi-Grancher, P. Lavalle, C. Frochot, M.-L. Viriot, S. Muller and X. Wang, *Bio-Medical Materials and Engineering*, 2006, **16**, 131.
5 J. Venugopal, Y. Z. Zhang and S. Ramakrishna, *Nanotechnology: (Bristol, Print)*, 2005, **16**, 2138.
6 Y. Mohammadi, M. Soleimani, M. Fallahi-Sichani, A. Gazme, V. Haddadi-Asl, E. Arefian, J. Kiani, R. Moradi, A. Atashi and N. Ahmadbeigi, *International Journal of Artificial Organs*, 2007, **30**, 204.
7 S. Gu, *Gaofenzi Tongbao*, 2005, **2**, 13.
8 W. J. Cho, J. H. Kim, S. H. Oh and J. H. Lee, *Key Engineering Materials*, 2007, **342–343** (*Advanced Biomaterials VII*), 293.
9 V. Pornsopone, P. Supaphol, R. Rangkupan and S. Tantayanon, *J. Polym. Res.*, 2007, **14**, 53.
10 I. C. Liao, S. Y. Chew and K. W. Leong, *Nanomedicine*, 2006, **1**, 465.
11 Z. Huang and A. Yang, *Gaofenzi Xuebao*, 2006, **1**, 48.
12 S. Agarwal, S. Horst and M. Bognitzki, *Macromol. Mater. Eng*., 2006, **291**, 592.
13 J. T. McCann, M. Marquez and Y. Xia, *Nano Lett.*, 2006, **6**, 2868.
14 S.-H. Tan, R. Inai, M. Kotaki and S. Ramakrishna, *Polymer: (Guildf.)*, 2005, **46**, 6128.
15 Y. M. Shin, M. M. Hohman, M. P. Brenner and G. C. Rutledge, *Polymer*, 2001, **42**, 9955.
16 V. Hoffart, N. Ubrich, C. Simonin, V. Babak, C. Vigneron, M. Hoffman, T. Lecompte and P. Maincent, *Drug Dev. Ind. Pharm*., 2002, **28**, 1091.
17 Yu. V. Chernysheva, V. G. Babak, N. R. Kildeeva, F. Boury, J. P. Benoit, N. Ubrich and P. Maincent, *Mendeleev Commun.*, 2003, 65.
18 V. G. Babak, Yu. V. Chernysheva, N. R. Kildeeva, V. E. Tikhonov, F. Baros, D. Dumas, N. Ubrich and P. Maincent, *XII International Workshop on Bioencapsulation*, Vittoria, Spain, 2004, p. 41.
19 V. G. Babak, F. Baros, O. Boulanouar, F. Boury, M. Fromm, N. R. Kildeeva, N. Ubrich and P. Maincent, *Colloids Surf. B: Biointerfaces*, 2007, **59**, 194.
20 D. Dumas, L. Grossin, G. Cauchois, M. Gentils, R. Santus and J. F. Stoltz, *Biorheology*, 2003, **40**, 253.
21 P. Fievet, M. Sbai, A. Szymczyk and A. Vidonne, *J. Membr. Sci*., 2003, **226**, 227.
22 M. Sbai, A. Szymczyk, P. Fievet, A. Sorin, A. Vidonne, S. Pellet-Rostaing, A. Favre-Reguillon and M. Lemaire, *Langmuir*, 2003, **19**, 8867.
23 F. Yang, R. Murugan, S. Wang and S. Ramakrishna, *Biomaterials*, 2005, **26**, 2603.
24 S. Megelski, J. S. Stephens and C. D. Bruce, *Macromolecules*, 2002, **35**, 8456.
25 R. Inai, M. Kotaki and S. Ramakrishna, *Nanotechnology*, 2005, **16**, 208.
26 V. G. Babak, *La Gazette de l'APGI*, 1999, **16**, 7.
27 V. Babak, F. Baros, F. Boury, J. Desbrieres, H. Huilier, N. Kildeeva and P. Maincent, *4th World Congress on Emulsions*, Lyon, France, 2006, p. 270.
28 Y. Z. Zhang, X. Wang, Y. Feng, J. Li, C. T. Lim and S. Ramakrishna, *Biomacromolecules*, 2006, **7**, 1049.
29 Q. P. Pham, U. Sharma and A. G. Mikos, *Biomacromolecules*, 2006, **7**, 2796.
30 M. Zuwei, M. Kotaki and S. Ramakrishna, *J. Membr. Sci*., 2006, **272**, 179.
31 G. L. Jinming, L. Niklason and R. Langer, *J. Biomed. Mater. Res*., 1998, **42**, 417.
32 I. K. Kwon, K. D. Park, S. W. Choi, S.-H. Lee, E. B. Lee, J. S. Na, S. H. Kim and Y. H. Kim, *J. Biomater. Sci., Polym. Ed*., 2001, **12**, 1147.

Received: 15th October 2007; Com. 07/3029